

# OBSERVATION OF THE NONLINEAR SATURATION OF LANGMUIR WAVES DRIVEN BY PONDEROMOTIVE FORCE IN A LARGE-SCALE PLASMA

*R. K. Kirkwood*

*D. S. Montgomery\*\**

*B. B. Afeyan\**

*K. G. Estabrook*

## Introduction

The scattering of laser energy by large-amplitude Langmuir waves has long been recognized as an important loss mechanism in laser driven inertial confinement fusion (ICF) research.<sup>1</sup> The scattering waves are driven to large amplitude by the three-wave process of stimulated Raman scattering (SRS), in which the incident electromagnetic wave decays into a Langmuir wave and a scattered wave. Early modeling efforts assumed the three-wave process was limited by simple convective saturation, which results from the propagation of energy out of the interaction volume by the decay waves. In the large-scale plasmas expected in ignition experiments, however, the convective saturation level is sufficiently high that the stimulated Langmuir waves can be saturated at much lower amplitude by nonlinear processes, such as secondary stimulation of ion-acoustic, Langmuir, and electromagnetic waves.<sup>2-6</sup> The primary manifestation of nonlinear saturation is that the Langmuir-wave amplitude can no longer increase linearly with the ponderomotive force, but rather is limited to a lower, saturated level. Previous experiments have found evidence of secondary mechanisms and their effect on SRS.<sup>7-13</sup> More recent experiments have shown that, under conditions similar to what is expected under ignition conditions, the SRS reflectivity is dependent on the damping rate of the ion-acoustic wave,<sup>14-16</sup> consistent with saturation by secondary decay. Further, it has been shown that the scattered SRS spectrum has both a shape<sup>17</sup> and magnitude<sup>14</sup> that are consistent with Langmuir-wave saturation by a secondary decay involving ion waves. However, there was previously no direct observation of the nonlinear response of the Langmuir wave. The

potential to observe the Langmuir wave response has been shown by theoretical<sup>18,19</sup> and experimental<sup>13,20-22</sup> studies, in which Langmuir waves and their secondary decay products<sup>23</sup> have been generated by the beating of two laser beams of different frequency. A parallel line of experimentation using beating laser beams to excite ion waves<sup>24,25</sup> has succeeded in demonstrating that the response of the waves to ponderomotive force is linear.

We now report the first demonstration of the nonlinear saturation of Langmuir waves driven by ponderomotive force under conditions relevant to indirect-drive ignition experiments. The Langmuir waves are driven by the beating of two intersecting laser beams of widely disparate frequency. Scattering of energy from the high-frequency beam to the low-frequency beam provides a measure of the wave amplitude, while adjustment of the intensity of the low-frequency beam allows the ponderomotive force to be varied. The amplitude of the Langmuir wave is thus found to be very weakly dependent on the ponderomotive drive when the drive is large, as expected by secondary decay models.<sup>2-6</sup> The experiments are done in low-Z plasmas, which have electron temperatures, densities, and scale length similar to what is expected in indirect-drive ignition experiments<sup>26,27</sup> and which support the interpretation of the observed dependence of SRS reflectivity on the damping rate of the ion-acoustic wave<sup>14,15,16</sup> as due to saturation by secondary decay under these conditions.

## Description of the Experiments

The experiments were performed at the ten-beam Nova laser facility, using eight of the beams to preheat a gas-filled target and the remaining two beams as interaction beams. The target consists of a 0.3- $\mu\text{m}$ -thick polyimide bag that is filled with atmospheric pressure gas so that it is nearly spherical, with a radius of 1.3 mm, when placed in the vacuum chamber. The target is preheated

\*Polymath Associates, Livermore, CA, and University of Nevada, Reno, Reno, NV

\*\*Los Alamos National Laboratory, Los Alamos, NM

with eight of the  $f/4.3$  beams that are defocused (converging) to a diameter of  $\sim 1.7$  mm. The heater beams each deliver 2.5 kJ at a wavelength of 351 nm in a 1-ns square pulse that produces a plasma that is hot and relatively homogeneous in the region inside a 1-mm radius and during the latter half of the heating pulse (0.5 to 1.0 ns). The target is filled to between 730 and 800 T with a mixture of the following gases:  $C_3H_8$ ,  $C_5H_{12}$ ,  $CH_4$ , and a 1% Ar impurity to allow for x-ray spectral analysis.<sup>26</sup> The three carbonous gases are mixed in various percentages, which together with small variations in the fill pressure allows the density of electrons to be controlled, thus allowing adjustment of the Langmuir-wave resonance. Application of the heater beams for a duration of 1.0 ns results in a plasma with an electron density approximately that of the initial gas fill ( $n_0$ ) inside a radius of  $\sim 1$  mm and an electron temperature that increases to a maximum of  $\sim 2.6$  keV at 1.0 ns. The electron temperature is determined from x-ray spectral measurements from a region of plasma at  $r = 400 \mu\text{m}$ , and its peak value is in reasonable agreement with LASNEX simulations.<sup>26</sup>

The remaining two beams are focused in the interior of the plasma and brought to best focus at the same point at  $r = 400 \mu\text{m}$ , where the plasma is expected to be most uniform. The beams are chosen to cross  $25^\circ$  away from antiparallel, approximating the geometry of SRS backscatter.<sup>27</sup> The pump beam is  $f/4.3$  with 2.5 kJ of energy at a wavelength of 351 nm in a 1-ns square pulse that is delayed 0.5 ns with respect to the heaters. The use of a random phase plate (RPP) on the pump beam limits the spot size to  $320\text{-}\mu\text{m}$  full width at half maximum (FWHM) at best focus. The probe beam has a wavelength of 527 nm with a variable energy (100 J to 1 kJ) in a 2-ns pulse that is turned on simultaneously with the heaters. The RPP on the probe limits the spot size to  $350 \mu\text{m}$ . This allows the beams to interact in a parallelogram  $800 \mu\text{m}$  on each side with an acute interior angle of  $25^\circ$  as shown in Figure 1. The timing of the beams allows the interaction to occur during the 0.5- to 1.5-ns period. During the first half of this period, the plasma is being heated, while during the second half the plasma is being cooled by radiation and expansion. The transmitted power of the probe beam is collected by a scatter plate of roughened fused silica. The plate is imaged onto a gated optical imager and onto the cathode of a photodiode that provides a measure of the transmitted probe power as a function of time.<sup>28</sup> The response time of the photodiode measurements is improved to 150 ps by deconvolving the measured impulse response of the system.

Measurements of the transmission of the probe beam were performed over a range of plasma densities and compared with the transmission from experiments under the same conditions with no pump beam. The initial density in each experiment was determined by differing gas fill pressures and molecular composition. The initial density was varied from 5.6% to 8.2% of the critical density

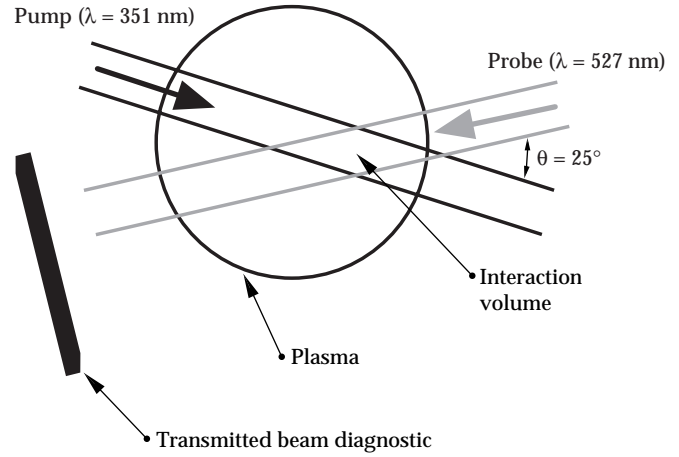


FIGURE 1. Geometry of the crossing beam experiment showing a short wavelength, high-intensity pump beam and a long wavelength, low-intensity probe beam intersecting in a spherical, low-density plasma. The transmitted beam diagnostic measures the time history of the transmitted power of the probe beam. (08-00-0798-1537pb01)

for 351 nm light ( $n_{c0}$ ), which brackets the Langmuir-wave resonance in this case. The plasma density during the 0.5- to 1.0-ns interaction period is very close to the initial density over this range, as expected from LASNEX simulations<sup>27</sup> and confirmed by the measurements of the peak wavelength of SRS back<sup>27</sup> and forward<sup>28</sup> scattering. The transmitted probe power in the absence of a pump beam (pump-off) was only weakly sensitive to the changes in density, while the transmitted power in the presence of the pump beam (pump-on) was observed to have a substantial enhancement compared to the pump-off case when the initial plasma density was in the vicinity of  $n_0/n_{c0} = 7.1\%$ . Figure 2 shows the time history of

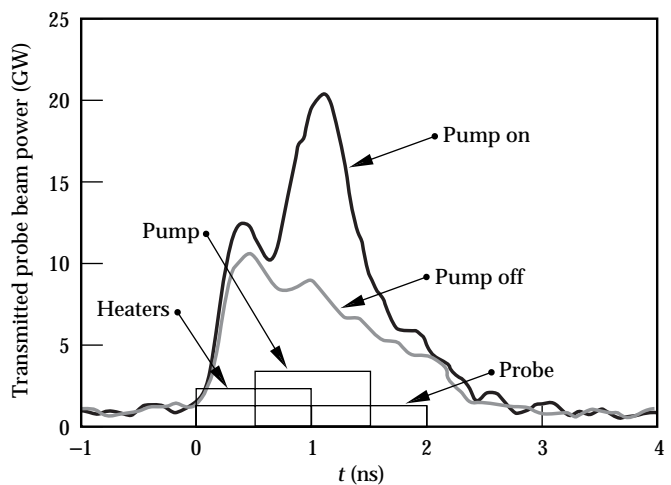


FIGURE 2. Power transmitted through the plasma by the probe beam for the cases with and without a pump beam. The transmission of the probe beam is enhanced by a factor of  $\geq 2$  during the period in which the pump is on, indicating that a large amplitude Langmuir wave is being stimulated and is scattering substantial energy. (08-00-0798-1538pb01)

the transmitted probe power near the resonant value of density for both the pump-on and pump-off cases. The observed attenuation of the transmitted beam in the pump-off case is determined primarily by inverse bremsstrahlung absorption and is also affected by scattering, as described in Moody.<sup>28</sup> In the pump-on case, the probe transmission is observed to be strongly enhanced during the 0.5- to 1.5-ns window when both pump and probe are on, indicating that significant energy is transferred from the pump beam. The amplification is measured during the 0.5- to 1.0-ns period by averaging the transmitted power over this period and taking the ratio of the average power in the pump-on case to that in the pump-off case. This amplification is  $2.15 (\pm 0.3)$  for the case shown in Figure 2. Spectral measurements of the transmitted power in the pump-on experiment show a very narrow line width ( $\leq 2$  nm). The interaction is found to be strongly resonant with plasma density, as observed in the plot of amplification vs  $n_0$  shown in Figure 3. The data in Figure 3 is restricted to the case of low probe-beam power ( $P \leq 0.2$  TW), so that the wave response is small and unsaturated. The observation of maximum amplification at 7.1% of the critical density combined with the observation of little or no effect of the pump (amplification  $\sim 1$ ) at both higher and lower density in Figure 3

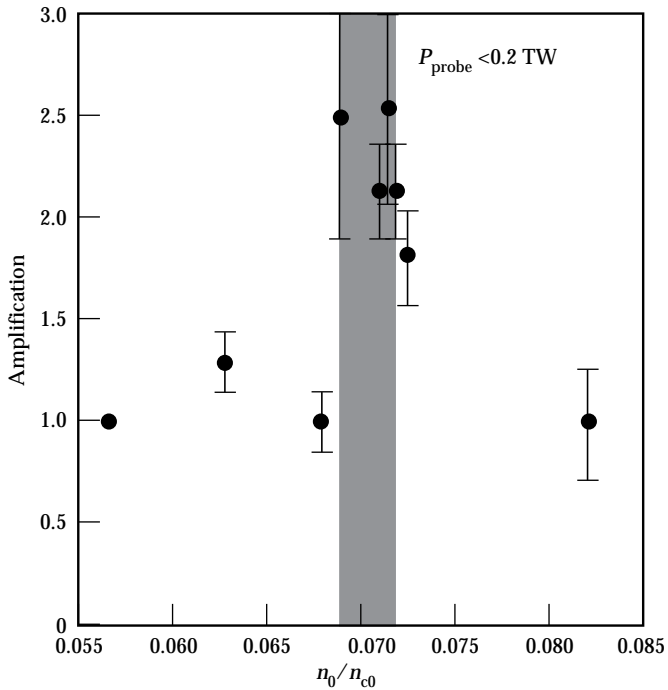


FIGURE 3. The amplification measured during the 0.5- to 1.0-ns period shown as a function of the initial plasma density for the case of low probe intensity and strong ion-acoustic wave damping (i.e., unsaturated Langmuir waves). A maximum is observed at  $n_0/n_{c0} = 7.1 (\pm 0.15\%)$  (shaded), consistent with the Langmuir resonance. (08-00-0798-1539pb01)

are consistent with the calculated Langmuir-wave resonance for a plasma with an electron temperature of 2.1 keV, which is somewhat lower than the peak value<sup>26</sup> and is consistent with the average temperature measured during the 0.5- to 1.0-ns period. The data in Figure 3 supports the interpretation that the amplification is due to a resonant three-wave interaction of the two beams with a Langmuir wave in the plasma.

Having identified a density resonant with the Langmuir wave in this experiment ( $n/n_c = 7.1\%$ ) and determined the magnitude of the amplification when the Langmuir-wave amplitude is small, we performed experiments to investigate the nonlinear response of Langmuir waves at larger amplitudes by increasing the probe-beam intensity. These experiments show that the amplification is substantially reduced by increasing the probe intensity, while holding the plasma density close to the resonant value (i.e., within the shaded region in Figure 3). For example, the amplification observed at low probe power (65 GW) under the conditions of Figure 2 is  $2.5 \pm 0.5$ , while the amplification in a similar experiment with a probe power of 500 GW is less than  $1.32 \pm 0.12$  (where 1.0 represents no resonance). The nonlinearity is not due to the transmission diagnostic, which has been calibrated and found to be linear with up to an order-of-magnitude-higher transmitted power.<sup>28</sup> These observations are used to demonstrate the saturation of the Langmuir wave by interpreting the enhancement of the probe beam as a measurement of the Langmuir-wave amplitude and the product of the incident intensities of the probe and pump beams as the ponderomotive force that drives the Langmuir wave. This analysis can be understood by considering the total power scattered from the pump beam rather than the amplification of the probe. The power scattered from the pump is determined as the difference between the transmitted probe power with the pump on and with the pump off, again averaging over the 0.5- to 1.0-ns period when all the beams are on. This scattered power is corrected for absorption between the point of scattering (where the center of the beams cross) and the outer edge of the plasma and is plotted vs the incident probe power with the pump power constant in Figure 4. Because the power scattered by the Langmuir wave is proportional to the square of its amplitude  $\delta n^2$ , and because the probe-beam intensity is proportional to the square of the ponderomotive force driving the Langmuir wave, a linear Langmuir wave response would be represented by data that parallels the linear scaling curve shown as a black line in Figure 4. Clearly, the scattered power falls below the linear scaling when the probe power is greater than 200 GW, demonstrating that the Langmuir-wave amplitude is nonlinearly saturated at high ponderomotive drive. This observation of the nonlinearly saturated response of the Langmuir wave to the ponderomotive force produced by the beating of

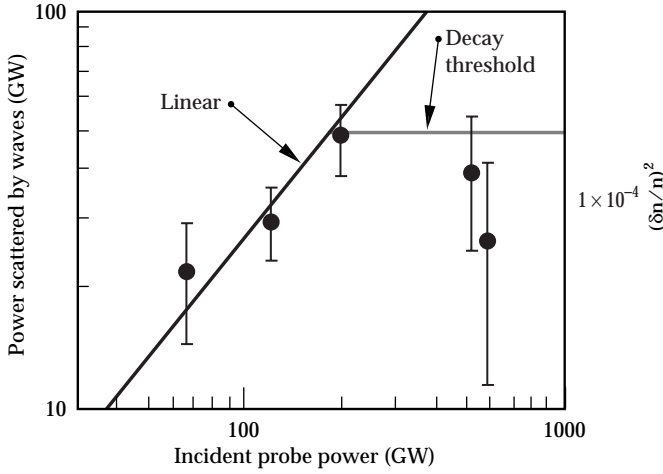


FIGURE 4. The additional power scattered into the probe beam (scattered power) when the pump beam is present and the density is resonant, plotted vs the incident power in the probe. The black line represents a linear relationship between the amplitude of the scattering Langmuir wave and the probe power (ponderomotive force), which is fit to the data for low probe power. The data at high probe power is below the linear scaling (i.e., saturated). The scattered power is interpreted as Langmuir-wave amplitude, and the gray line represents the threshold of the secondary decay instability, as discussed in the text. (08-00-0798-1540pb01)

the two laser beams is the primary result of this article. Such a nonlinearity may be created by many mechanisms, ranging from nonlinear Landau damping, to the relativistic detuning that has been studied in high-phase-velocity plasma waves,<sup>21</sup> to the secondary decay of the Langmuir wave<sup>2-6</sup> and as such is consistent with previous interpretations of data from ignition-relevant plasmas that suggest that SRS backscatter is limited by saturation by secondary decays involving ion waves.<sup>14,15</sup>

The structure of the spectrum of transmitted light and scattering waves was studied in a further set of experiments. These experiments studied the interaction of the two beams during the 1.15- to 1.5-ns period, after the heater beams shut off, to eliminate spectral contributions from heater side scatter. The transmitted probe beam was analyzed by a high-resolution spectrometer for cases corresponding to incident probe powers of 50, 200, and 450 GW in Figure 4. In all cases the spectrum was less than 0.6-nm FWHM, corresponding to a Langmuir-wave spectrum with a width of  $\Delta\omega/\omega = 5 \times 10^{-3}$ . Amplification of the probe beam was clearly observed in the lowest-power experiment and diminished in higher-power experiments. This is consistent with the early time measurements of Figure 4. This data cannot be directly compared with the data in Figure 4, however, because the absence of heaters during this period makes the plasma conditions and their time dependence different than during the early period. The observed Langmuir-wave spectrum is much narrower than expected for a cascade of

multiple Langmuir decay instabilities (LDIs), indicating that if such a cascade is present, it involves very little energy. Because of the geometry and wavelength of the measurements, the transmitted spectrum provides information only about Langmuir waves that are copropagating with the primary Langmuir wave, and it may be consistent with either saturation by a single Langmuir decay producing a counterpropagating wave<sup>8,9</sup> or with saturation by the electromagnetic decay instability (EDI) in which the decay products are not Langmuir waves.

## Comparison with Secondary Decay Model

A comparison of the observations with theories of secondary decay of the Langmuir wave<sup>2-6</sup> can be made by estimating the amplitude of the waves from the fraction of power they scatter from the pump beam. Such an estimate is made using a 1D, Bragg wave scattering model for a homogeneous beam,<sup>14,29</sup> which gives an estimate of the scattering wave amplitude. This model gives the relationship between the fraction of pump power scattered  $F$  and the wave amplitude  $(\delta n/n)$  in terms of the normalized plasma density, the incident-beam wave number, and two characteristic lengths (the system size  $L$  and the correlation length of the Langmuir waves  $\Delta k$ )<sup>-1</sup>.

$$F \approx \frac{1}{4} \left( \frac{n}{n_{c0}} \right)^2 k_0^2 L (\Delta k)^{-1} \left( \frac{\delta n}{n} \right)^2 \quad (1)$$

As an estimate of the correlation length, we use the correlation length of the driving ponderomotive force produced by the two  $f/4.3$  beams. The width of the spectrum of  $k_z = (\mathbf{k}_1 - \mathbf{k}_2) \cdot \hat{z}$  is the speckle length projected into the axis of the beam ( $\hat{z}$ ). We use this width of the  $k_z$  spectrum of the incident beams as an estimate of the correlation length of the Langmuir waves:  $\Delta k \approx 1.2 \times 10^6 \text{ m}^{-1}$ . Using this length and the experimental plasma parameters in Eq. 1, we estimate the amplitude of the scattering Langmuir wave from the measurements of the fraction of pump-beam power that the wave scatters, as shown on the right axis in Figure 4. This fraction is calculated using the pump-beam power determined from the incident power and a correction for inverse bremsstrahlung between the plasma edge and the point at which the centers of the two beams cross. The results are compared with the threshold for the secondary decay instability, shown as the gray line in Figure 4. The threshold is determined by the damping rates of the secondary decay products and

can be written in terms of the Langmuir-wave amplitude as

$$\left(\frac{\delta n}{n}\right) = 4 k_L \lambda_D \left(\frac{v_{ia}}{\omega_{ia}}\right)^{1/2} \left(\frac{v_3}{\omega_3}\right)^{1/2} \quad (2)$$

where  $k_L$  is the wave number of the primary Langmuir wave driven by the beating of the two beams,  $\lambda_D$  is the Debye length,  $\omega_{ia}$  and  $v_{ia}$  are the real and imaginary parts of the frequency of the ion-acoustic decay product ( $v_{ia}/\omega_{ia} \approx 0.2$  for a  $T_{ion}/T_e \approx 0.15$  as determined by simulations for this case<sup>30</sup>), and  $\omega_3$  and  $v_3$  represent the frequency of the third wave.

When the instability is EDI, the third wave is an electromagnetic wave,<sup>6</sup> and  $\omega_3$  and  $v_3$  are approximately the plasma frequency and the inverse bremsstrahlung absorption rate. When the instability is LDI, the third wave is a Langmuir wave, and  $\omega_3$  and  $v_3$  are approximately the plasma frequency and the electron Landau damping rate. Electrons are produced in these plasmas by mechanisms such as collisional absorption of the beams, nonlinear Landau damping of the Langmuir waves, and nonlocal heat transport.<sup>31</sup> Recent analysis of the non-Maxwellian velocity distribution of such electrons has shown that the electron Landau damping rate may be much lower than in a Maxwellian plasma. In a laser hot spot the damping rate could be reduced by an order of magnitude, approaching the collisional damping rate as a lower limit. As a result, a necessary condition for the presence of EDI or LDI in a non-Maxwellian plasma is that the  $\delta n/n$  estimated from the measured scattered power (points in Figure 4) be greater than or equal to the threshold given by Eq. 2 evaluated with  $\omega_3$  and  $v_3$  equal to the plasma frequency and the collisional damping rate (gray line in Figure 4). This threshold is found to be close to the observed saturation level in Figure 4. This is consistent with previous interpretations<sup>2-6, 14-16</sup> that the Langmuir wave is saturated by a secondary decay process involving ion waves.

## Conclusion

We have developed a technique to study the properties of Langmuir waves in ignition-relevant plasmas and used this technique to demonstrate that the response of Langmuir waves to ponderomotive force is nonlinearly saturated consistent with earlier studies of SRS.<sup>14,15</sup>

## Acknowledgments

The authors gratefully acknowledge conversations with D. F. DuBois (Los Alamos National Laboratory) and W. Rozmus (University of Alberta) on the nature of EDIs and LDIs, as well as with T. Johnston (INRS). This work was performed with support from the Science Use of Nova program.

## Notes and References

1. See for example W. L. Kruer, *The Physics of Laser Plasma Interactions* (Addison-Wesley Publishing Co., Redwood City, CA, 1988).
2. S. J. Karttunen, *Plasma Physics* **22**, 151 (1980).
3. G. Bonnaud, Denis Pesme, and Rene Pellat, *Phys. Fluids B* **2**, 1618 (1990).
4. B. Bezzerides, D. F. Dubois, and H. A. Rose, *Phys. Rev. Lett.* **70**, 2569 (1993).
5. T. Kolber, W. Rozmus, and V. T. Tikhonchuk, *Phys. Fluids B* **5**, 138 (1993).
6. K. L. Baker, Ph.D. Dissertation, University of California, Davis, 1996; see also P. K. Shukla et al., *Phys. Rev. A* **27**, 552 (1983).
7. D. M. Villeneuve et al., *Phys. Rev. Lett.* **71**, 368 (1993).
8. K. L. Baker et al., *Phys. Rev. Lett.* **77**, 67 (1996).
9. C. Labaune et al., *Phys. of Plasmas* **5**, 234 (1998).
10. C. J. Walsh, D. M. Villeneuve, and H. A. Baldis, *Phys. Rev. Lett.* **53**, 1445 (1984).
11. H. A. Baldis et al., *Phys. Rev. Lett.* **62**, 2829 (1989).
12. D. S. Montgomery et al., submitted to *Phys. Rev. Lett.*
13. D. Umstadter, W. B. Mori, and C. Joshi, *Phys. Fluids B* **1**, 183 (1989).
14. R. K. Kirkwood et al., *Phys. Rev. Lett.* **77**, 2706 (1996).
15. J. C. Fernandez et al., *Phys. Rev. Lett.* **77**, 2702 (1996).
16. R. K. Kirkwood et al., *Physics of Plasmas* **4**, 1800 (1997).
17. R. P. Drake and S. H. Batha, *Phys. of Fluids B* **3**, 2936 (1991).
18. N. Kroll, A. Ron, and N. Rostoker, *Phys. Rev. Lett.* **13**, 83 (1964).
19. A. N. Kaufman and B. I. Cohen, *Phys. Rev. Lett.* **30**, 1306 (1973).
20. B. L. Stansfield, R. Nodwell and J. Meyer, *Phys. Rev. Lett.* **26**, 1219 (1971).
21. C. E. Clayton, C. Joshi, C. Darrow, and D. Umstadter, *Phys. Rev. Lett.* **54**, 2343 (1985).
22. C. Darrow et al., *Phys. Rev. Lett.* **56**, 2629 (1986).
23. F. Amiranoff et al., *Phys. Rev. Lett.* **68**, 3710 (1992).
24. R. K. Kirkwood et al., *Phys. Rev. Lett.* **77**, 2065 (1996); and *ICF Quarterly Report* **6**(2), Lawrence Livermore National Laboratory, Livermore, CA (UCRL-LR-105821-96-2).
25. W. L. Kruer, B. B. Afeyan, S. C. Wilks, and R. K. Kirkwood, *Physics of Plasmas* **3**, 382 (1996).
26. S. H. Glenzer et al., *Phys. Rev. E* **55**, 927 (1997).
27. B. J. MacGowan et al., *Physics of Plasmas* **3**, 2029 (1996).
28. J. D. Moody et al., *Rev. Sci. Instr.* **68**, 1725 (1997).
29. T. Kolber, W. Rozmus, and V. T. Tikhonchuk, *Phys. Plasmas* **2**, 256 (1995).
30. E. A. Williams et al., *Physics of Plasmas* **2**, 129 (1995).
31. B. B. Afeyan et al., *Phys. Rev. Lett.* **80**, 2322 (1998), and elsewhere in this volume.